

The Propagation of Ultrasonic Waves in Gas-containing Suspensions

The Propagation of Ultrasonic Waves in Gas-containing Suspensions

By

Volodymyr Morkun,
Natalia Morkun
and Andrii Pikilniak

Cambridge
Scholars
Publishing



The Propagation of Ultrasonic Waves in Gas-containing Suspensions

By Volodymyr Morkun, Natalia Morkun and Andrii Pikilniak

This book first published 2019

Cambridge Scholars Publishing

Lady Stephenson Library, Newcastle upon Tyne, NE6 2PA, UK

British Library Cataloguing in Publication Data

A catalogue record for this book is available from the British Library

Copyright © 2019 by Volodymyr Morkun, Natalia Morkun
and Andrii Pikilniak

All rights for this book reserved. No part of this book may be reproduced, stored in a retrieval system, or transmitted, in any form or by any means, electronic, mechanical, photocopying, recording or otherwise, without the prior permission of the copyright owner.

ISBN (10): 1-5275-1814-0

ISBN (13): 978-1-5275-1814-8

TABLE OF CONTENTS

List of Figures.....	vii
Preface.....	xi
Chapter One.....	1
Volume Ultrasonic Oscillations Propagation in Gas-Containing Suspensions	
1.1. Introduction.....	1
1.2. The calculation of the ultrasound absorption and scattering cross-sections on the solid particles and gas bubbles suspended in a liquid.....	4
1.3. Laws of fluctuations influence of the number and size of particles, which are suspended in a liquid on the ultrasonic field characteristics.....	8
1.4. Evaluation of the scattered ultrasonic waves intensity.....	17
1.5. The influence laws of the ultrasound velocity dispersion in the liquid on the characteristics of the acoustic vibrations final pulse.....	20
1.6. The reflection of volume ultrasonic waves from the inhomogeneous surface.	24
Chapter Two.....	27
The Study of Lamb Waves Propagation on the Plate which Contacts with the Gas-containing Iron Ore Pulp	
2.1. The main elements of the theory of Lamb waves propagation in the plate.....	27
2.2. Theoretical foundations of Lamb wave propagation along the plate in contact with the gas-containing suspension.....	31
Chapter Three.....	43
The Propagation of Volume Ultrasonic Waves and Lamb Waves in the Presence of a Magnetic Field	

Chapter Four.....	61
The Love Waves Propagation in Contact with Heterophase Media under the Magnetic Field Influence	
4.1. Introduction.....	61
4.2. The Love waves propagation in a layer, which is in contact with the process fluid	76
4.2.1. The Love waves propagation in contact with the solid phase process medium	77
4.2.2. The Love waves propagation in contact with the liquid- phase process fluid.....	79
4.3. The influence of magnetic field on the elastic waves propagation in a solid medium	84
 Chapter Five	 95
Ultrasonic Control of Solid Phase Concentration and Granulometric Composition of the Crushed Material in the Pulp Flow	
5.1. The theoretical fundamentals of ultrasonic testing of the industrial suspensions main characteristics.....	95
5.2. Ultrasonic control of minerals disclosure degree during ore grinding	103
5.3. Ultrasonic monitoring of quantitative characteristics of pulp flows.....	124
 References	 127

LIST OF FIGURES

- Figure 1-1: The dependence of the ultrasound absorption and scattering cross-sections on suspended particles on the oscillation frequency.
- Figure 1-2: The function of air bubble size distribution.
- Figure 1-3: The dependence of the ultrasonic attenuation cross-section by air bubbles on the sound wave frequency.
- Figure 1-4: Spatial orientation of the disc ultrasonic vibrations transducer.
- Figure 1-5: Geometrical interpretation of the measuring channel.
- Figure 1-6: The dependence of α_λ on the frequency for the different parameters of beta distribution.
- Figure 1-7: The dependence of α_λ on the frequency for various values of concentration n .
- Figure 1-8: The dependence of α_λ on the frequency for various values of average particle radius.
- Figure 1-9: The dependence of α_λ on the average radius of suspended particles for various ultrasonic oscillations frequencies.
- Figure 1-10: The dependence of frequency components σ_i on the ultrasonic oscillations frequency.
- Figure 1-11: The dependence of the asymptotic values of the accumulation factor on the ultrasonic oscillations frequency.
- Figure 1-12: The change of the acoustic oscillations pulse parameters under the dispersive medium influence.
- Figure 1-13: Pulse type of acoustic oscillations, which are passed through a controlled volume of pulp.
- Figure 2-1: Lamb wave phase velocity of Aluminium-2024-T3.
- Figure 2-2: Tuning of Aluminium-2024-T3 2mm: Strain.
- Figure 2-3: Lamb wave group velocity of Aluminium-2024-T3.
- Figure 2-4: Lamb wavelength of Aluminium-2024-T3.
- Figure 2-5: The dependence of the attenuation coefficient on the Lamb wavelength for the medium parameters.
- Figure 2-6: The dependence of the relative change in the Lamb waves velocity on the medium parameters.
- Figure 2-7: Geometrical interpretation of the measuring channel.
- Figure 3-1: Geometric interpretation of the measuring channel.

Figure 3-2: The frequency dependence of ultrasound absorption in the pulp in a magnetic field.

Figure 3-3: The dependence of F on $f \cdot f_m^{-1}$ in pulp.

Figure 3-4: The dependence of the ultrasonic attenuation in the pulp in the magnetic field on $\sin^2\theta$.

Figure 3-5: The movement of the pulp iron ore particles in a magnetic field.

Figure 3-6: The graph of the function $erf(\xi)$.

Figure 4-1: Scheme of Love waves propagation.

Figure 4-2: The influence of ratio between densities of media 1 and 2 on the dispersion.

Figure 4-3: The influence of the layer density on the dispersion of Love waves.

Figure 4-4: The influence of film thickness on the dispersion of Love waves.

Figure 4-5: The dependence of Love waves phase velocity on the film thickness at different ratios between the density of the medium 1 and 2.

Figure 4-6: The dependencies of intensity I_1 on ρ_1 ($\rho_1 > \rho_2$) for the different values of frequency ω .

Figure 4-7: The dependencies of intensity I_1 on ρ_1 ($\rho_2 > \rho_1$) for the different values of frequency ω .

Figure 4-8: The dependencies of intensity I_2 on ρ_1 ($\rho_1 > \rho_2$) for the different values of frequency ω .

Figure 4-9: The dependencies of parameters I_2 on z for values h .

Figure 4-10: The dependencies of intensity I_1 on h for the different values of ρ_1 .

Figure 4-11: The dependencies of parameters I_2 on h for the different values of ρ_1 .

Figure 4-12: The dependencies of parameters I_2 on ω for the different values of ρ_1 .

Figure 4-13: A system in which the elastic waves are propagated.

Figure 4-14: The dependence of $\lg y$, on the wave amplitude for liquid density.

Figure 4-15: The diagram of induced currents \vec{j} and fields \vec{E} arising in a conducting medium which moving with a velocity of \vec{V}_0 in a magnetic field with induction of \vec{B} .

Figure 5-1: The measurement of pulp solid phase particle size distribution.

Figure 5-2: The dependence of ω_r on the particle size of r size control class.

Figure 5-3: Calibration curves for the different particle size classes.

Figure 5-4: The dependence of $S' = f(\omega_{.74})$.

Figure 5-5: The particle motion in the intensive ultrasound field.

Figure 5-6: The dependence of the signal S_1/S_0 on the value aZ_0 under the fixed values $\langle \beta t \rangle$.

Figure 5-7 The dependence of the signal S_1/S_0 on the value $\langle \beta t \rangle$ under the fixed values aZ_0 .

Figure: 5-8 The block diagram of a measuring channel based on gamma radiation.

Figure: 5-9 Scheme of installation.

Figure: 5-10 The smoothed time dependence of the signal change.

Figure: 5-11 Time dependence of the generated signal for the different ore types.

Figure: 5-12. The cumulative curves of investigated types of ores.

Figure: 5-13 The calibration dependence of the useful component content for various time points.

Figure: 5-14 The installation scheme of the useful component disclosure degree determining.

PREFACE

The cost price of the raw material for the production of ferrous and non-ferrous metals in recent years is gradually increasing, for some objective reasons, but the content of the useful components in the ore for beneficiation is reducing.

Under these conditions, the issues, which are related to the improvement of minerals beneficiation process control through the introduction of modern high-performance automatic control and regulation systems, become crucial.

The grinding process stage is an intermediate link in the technological line of mineral processing, however, despite this, it has a decisive influence on the course of subsequent operations and the final performance of the entire concentrating plant.

The operating costs for ore grinding during beneficiation are up to 50% of the final product costs. The power consumption for grinding, depending on the quality of the initial ore and its final size, is in the range of 55% to 70% of the total electricity consumption of the plant.

The final performance indicators of the grinding process stage depend on the efficiency of the automatic control of grinding and classifying aggregates, which is determined primarily by the quality of information and algorithmic support in conditions of changing characteristics of the initial ore, and the technological equipment condition.

In the pulp density automatic stabilisation, the content control class size in classifying apparatuses discharge varies within $\pm 5\%$ with a period of about two hours. At present, the systems for automatic stabilisation of the pulp solid phase fineness (for example, based on a granulometer) have been developed, which make it possible to reduce the oscillations by $\pm 1.5\%$. As a result, the average content of the control class in the feed of the concentrating apparatus can be increased. Thus, the extraction of the useful component into the concentrate can also be increased, or if the granulometric composition of the grinding cycle output product is maintained, the volumes of processing ore are increased. Both ways lead to an additional amount of the useful component.

However, continuous monitoring of the useful component disclosure degree in the ore grinding is required, even when using the automatic stabilisation system of the composition, since their qualitative composition

varies. This circumstance requires corresponding changes of a reference value in the granulometry auto-stabilisation system. Otherwise, there are losses, due to an unreasonably high fineness (increased electricity consumption, increased wear of grinding bodies and mill liners, etc.), or due to insufficient grinding and incomplete minerals disclosure, associated with this (useful component losses increase in the concentrating devices tailings).

The existing facilities for operational control of the qualitative and quantitative characteristics of the crushed materials do not meet modern requirements.

A number of the most important chemical-mineralogical and physical-mechanical characteristics of the pulp solid phase, including the mineral disclosure degree during ore grinding, are not used to control the technological process, since there are no devices for their determination.

In this monograph, to solve such problems, the use of volume ultrasonic waves and surface Lamb and Love waves is proposed.

The principles and devices which are developed by these principles make it possible to improve the efficiency of automatic control of the ore grinding-classification processes, which is especially important for the Ukrainian economy, since in conditions of acute energy shortage, it allows the increase of the useful component extraction in concentrate, reduces operating costs, and thereby reduces the cost of final products, and increases its competitiveness in the world market, within the existing capacities of mining enterprises.

CHAPTER ONE

VOLUME ULTRASONIC OSCILLATIONS PROPAGATION IN GAS-CONTAINING SUSPENSIONS

1.1. Introduction

Ultrasonic methods have become a part of the research, measurement, and control arsenal, in various branches of science and industry [1, 2].

Ultrasonic oscillations are the periodic disturbances of the medium elastic state, characterised by a change in its physical properties, which occur synchronously with perturbation. During ultrasonic propagation, the local medium volume oscillations are transmitted to adjacent areas using elastic waves, which are characterised by a change in the medium density in space, and transfer of the fluctuations energy.

The basic relations describing the ultrasonic oscillations and waves in the medium follow from the equation of medium condition, Newton's equations of motion, and the continuity equation [3]. The result is wave-type equations which can be solved with the appropriate initial and boundary conditions.

Let's introduce the differential characteristic $I_\lambda(\vec{r}, \vec{\Omega})$ to describe the ultrasonic waves radiation field. By $I_\lambda(\vec{r}, \vec{\Omega})$ we denote the intensity of the ultrasonic wave (with a wavelength λ), which is defined as a radiation power per solid angle unit, which passes through a unit area perpendicular to the direction $\vec{\Omega}$ of the point \vec{r} . Here, $\vec{\Omega}$ is a unit vector, defining the direction in space, and \vec{r} is a radius vector, defining the position of a given point in space.

The purpose is to study the volume ultrasonic waves propagation in the gas-containing iron ore pulp, defining ultrasonic field characteristics in a liquid medium, which contains the solid particles and gas bubbles, and the influence of laws of fluctuations of the particles suspended in a liquid on the performance of the ultrasonic field.

There are irreversible losses of energy during propagation of acoustic waves in the liquid. They are caused by internal friction (viscosity), and, to some extent, by the thermal conductivity of the medium.

The expression for the plane wave absorption in the liquid, depending on the medium viscosity, was obtained in the works of Stokes, and the sound absorption coefficient due to the thermal conductivity of the medium is determined in the works of Kirchhoff and Bikar. [4].

The presence of solid particles and gas bubbles introduces some features to the process of ultrasonic wave energy attenuation and scattering.

The wave scattering on the solid phase particles becomes significant when the wavelength λ is commensurate with the size of the particles. The phase of waves, which are scattered in any given direction, and come from randomly located centres, is incoherent in the case when the wave passes through a medium containing a large number of randomly arranged particles.

Consequently, the total intensity of the ultrasonic wave at a given point is equal to the sum of the intensities of waves which are coming from all scattering centres. The scattering cross-sections, in this case, are additive, so the linear absorption and scattering coefficients can be determined by the formulas:

$$\begin{aligned}\Sigma_c(\lambda) &= n\sigma_c(\lambda); \\ \Sigma_s(\lambda) &= n\sigma_s(\lambda),\end{aligned}\tag{1.1}$$

where n is the particle concentration (number of particles per unit of volume); and $\sigma_c(\lambda)$ and $\sigma_s(\lambda)$ are the total cross-sections of the acoustic wave absorption and scattering on the particle.

The total cross-sections of absorption and scattering depend, not only on the wavelength of the ultrasonic vibration, but also on the particle size r . The values that determine the average fraction of the energy, which is absorbed and scattered by the medium per unit of path length and per unit of time, should be understood by a linear absorption and scattering coefficients.

The main characteristic of the ultrasonic radiation field $I_\lambda(\vec{r}, \vec{\Omega})$ must be determined from the kinematic equation. Before writing this equation, we should introduce the concept of the differential at the corners of the scattering coefficient:

$$\Sigma_s(\vec{\Omega} \rightarrow \vec{\Omega}') = n\sigma_s(\vec{\Omega} \rightarrow \vec{\Omega}'),\tag{1.2}$$

where $\sigma_s(\vec{\Omega} \rightarrow \vec{\Omega}')$ is a differential at the corners of energy scattering cross-section on the solid phase particle.

The value $\sigma_s(\vec{\Omega} \rightarrow \vec{\Omega}')$ represents a part of the energy, which is scattered by the particles in the element of a solid angle $d\vec{\Omega}'$. Obviously, the total scattering cross-section σ_s is associated with the differential scattering cross-section ratio:

$$\sigma_s = \int_{4\pi} \sigma_s(\vec{\Omega} \rightarrow \vec{\Omega}') d\vec{\Omega}'. \quad (1.3)$$

The kinetic equation, which is solved by function $I_\lambda(\vec{r}, \vec{\Omega})$, can be obtained by considering the energy balance in a volume element of the phase space:

$$\vec{\Omega} \nabla I_\lambda(\vec{r}, \vec{\Omega}) = -\Sigma(\lambda) I_\lambda(\vec{r}, \vec{\Omega}) + \int d\vec{\Omega}' \Sigma_s(\vec{\Omega}' \rightarrow \vec{\Omega}) I_\lambda(\vec{r}, \vec{\Omega}') + S_\lambda(\vec{r}, \vec{\Omega}), \quad (1.4)$$

where $\Sigma(\lambda) = \Sigma_c(\lambda) + \Sigma_s(\lambda)$; $S_\lambda(\vec{r}, \vec{\Omega})$ is the function of ultrasound source radiation density, which determines the average amount of energy, which is emitted per unit of time by a single phase volume.

The phase coordinates are the totality of variables r and Ω , while an elementary phase volume is determined by the product $d\vec{r} \cdot d\vec{\Omega}$.

The meaning of this equation is the following: The intensity variation of the ultrasonic beam, which has a direction $\vec{\Omega}$ at a point \vec{r} , occurs firstly, due to the beam attenuation-absorption and scattering (the first term on the right side), secondly, due to the scattering of the energy flux, which has previously had a direction $\vec{\Omega}'$ in the direction $\vec{\Omega}$ (the second term on the right side), and finally, due to the energy, which is coming to this beam from the sources (the last term on the right side). Equation (1.4) can be reduced to an integral equation of the form (1.5):

$$I_\lambda(\vec{r}, \vec{\Omega}) = \int d\vec{r}' \int d\vec{\Omega}' \Sigma_s(\vec{\Omega}' \rightarrow \vec{\Omega}) \frac{e^{-\tau(\vec{r}', \vec{r}, \lambda)}}{|\vec{r} - \vec{r}'|} \delta \left[\vec{\Omega} - \frac{(\vec{r} - \vec{r}')}{|\vec{r} - \vec{r}'|} \right] I_\lambda(\vec{r}', \vec{\Omega}') + I_\lambda^0(\vec{r}, \vec{\Omega}), \quad (1.5)$$

where $\tau(\vec{r}', \vec{r}, \lambda) = \Sigma(\lambda) |\vec{r} - \vec{r}'|$, $\delta(\cdot)$ is the Dirac delta function;

and $I_\lambda^0(\vec{r}, \vec{\Omega}) = \int_0^\infty S_\lambda(\vec{r} - \xi \vec{\Omega}, \vec{\Omega}) e^{-\tau(\xi, \lambda)} d\xi$ is the free term of the integral

equation (5), which determines the intensity of the unscattered ultrasonic wave; $\xi = |\vec{r} - \vec{r}'|$.

The solution of equation (1.5) can be written in the form of a Neumann series [5], which is the expansion of the ultrasonic waves scattering multiplicity solution. The first term of the Neumann series defines the ultrasonic waves non-scattered radiation field, while the second term defines the singly scattered radiation, etc.

However, it is impossible to obtain an expression analytically, even for the singly scattered radiation. Therefore, it is necessary to apply the numerical methods for integral equations solving of the form (1.5). One of the most common is the Monte Carlo method [6].

1.2. The calculation of the ultrasound absorption and scattering cross-sections on the solid particles and gas bubbles suspended in a liquid

The ultrasonic waves attenuation in water in the presence of the solid particles and air bubbles occurs mainly due to the wave energy absorption and scattering on the particles and bubbles. For a theoretical study of ultrasound propagation issues, it is necessary to know the corresponding sections of the absorption and scattering.

Let's assume, that there are solid particles with spherical radius r and density ρ_1 in water, then the absorption cross-section for such a particle is determined by the formula [4]:

$$\sigma_c(\lambda) = \frac{4\pi r^3}{3} k \left(\frac{\rho_1}{\rho_0} - 1 \right)^2 \frac{S}{S^2 + (\rho_1/\rho_0 + \tau)^2}, \quad (1.6)$$

where $k = 2\pi/\lambda$ is the wavenumber; ρ_0 is the fluid density; η is the fluid viscosity; ν is the ultrasonic wave frequency; $S = \frac{9}{4Br} \left(1 + \frac{1}{Br} \right)$;

$$B = (\pi\nu/\mu)^{\frac{1}{2}}; \quad \tau = \frac{1}{2} + \frac{9}{4Br}; \quad \mu = \eta/\rho_0.$$

The absorption cross-section determines the amount of energy, which is absorbed by the particle. These energy losses are caused by the presence of friction (viscosity) with the particle fluctuations.

The diffraction phenomena caused by the medium inhomogeneities (suspended particles) lead to sound waves energy dissipation. The cross-section of this process is given by:

$$\sigma_s(\lambda) = \frac{4\pi}{3} \cdot r^3 \cdot \frac{1}{6} k^4 \cdot r^3, \quad (1.7)$$

where k is the wavenumber; and r is the particle radius.

From (1.7) it is evident that $\sigma_s(\lambda) \propto 1/\lambda^4$, therefore with an increase of frequency the scattering cross-section increases $(\sigma_s) \sim \nu^4$.

The dependence of ultrasound absorption scattering and attenuation cross-sections on solid particles in the water on the frequency of the acoustic vibrations is shown in Fig. 1. The particle radius is 0.01cm. As can be seen from the figure, the ultrasound scattering becomes significant when the acoustic oscillations wavelength λ is comparable to the sizes of particles.

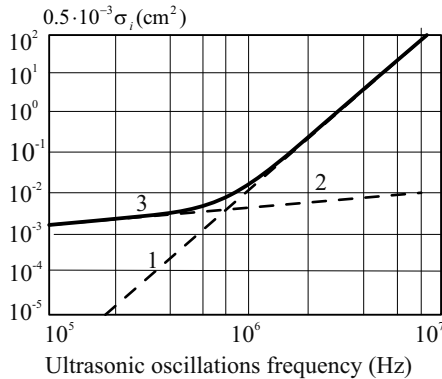


Fig. 1-1. The dependence of the ultrasound absorption and scattering cross-sections on suspended particles on the oscillation frequency: 1 - σ_s is the scattering cross-section; 2 - σ_a is the absorption cross-section; the particle radius $r = 0.01$ cm.

The presence of gas bubbles in the liquid also results in the absorption and scattering of acoustic energy. However, unlike the solid phase particles, the absorption and scattering by gas bubbles are resonant.

The main reasons for this phenomenon are as follows:

- a) the bubble heating and heat dissipation to the liquid, due to the bubble volume periodic changes which it undergoes under the influence of a sound wave;
- b) the scattering of the part of the sound energy, due to the fact that the oscillating bubble is a spherical sound transmitter;
- c) the energy losses due to the liquid flow formation around the oscillating bubble.

To characterise the acoustic waves absorption and scattering of oscillating gas bubbles, the concepts of the effective attenuation σ_p , absorption σ_c , and scattering σ_s cross-sections are introduced.

By the effective cross-section attenuation σ_p is meant the cross-sectional area perpendicular to the direction of the sound wave incidence, for which the incoming sound energy is equal to the energy sum, which is absorbed and scattered by the bubble.

The air bubbles absorption and scattering cross-sections are determined by the formulas:

$$\begin{aligned}\sigma_c &= \frac{4\pi R^2 (\delta/\eta - 1)}{(\nu_0^2/\nu^2 - 1)^2 + \delta^2}; \\ \sigma_s &= \frac{4\pi R^2 (\delta/\eta)}{(\nu_0^2/\nu^2 - 1)^2 + \delta^2},\end{aligned}\quad (1.8)$$

where ν_0 is the resonance frequency of the bubble with a radius R ; and δ is the attenuation constant; $\eta = 2\pi R/\lambda$.

From (1.8) we can see that the maximum values of the cross-sections are achieved by $\nu = \nu_0$.

The attenuation total cross-section is the sum of absorption and scattering cross-sections:

$$\sigma_p = \sigma_c + \sigma_s = \frac{4\pi R^2}{(\nu_0^2/\nu^2 - 1)^2 + \delta^2}. \quad (1.9)$$

In the case of air bubbles in the water, the resonant frequency can be estimated by the formula:

$$\nu_0 R = 0.328 \cdot 10^3 \text{ Hz} \cdot \text{cm}. \quad (1.10)$$

The value of the attenuation constant is dependent on the sound frequency. It ranges from 0.08 to 0.013 within a range of frequencies from 20 to 1000kHz [7].

Since the sound energy scattering and absorption by the air bubbles are resonant in this case, it is necessary for the ultrasonic waves attenuation calculation by air bubbles, to know not only the relevant attenuation cross-section, but also the function of air bubble size distribution.

Let's denote the bubble size distribution function by $f(R)$. Then the value $f(R)dR$ determines the number of bubbles with sizes in the range of R up to $R + dR$.

Based on the results of studies outlined in [8-11], the specific values of the air volume fraction in water, and the function of gas bubble size distribution, were chosen.

The values of the function $f(R)$, which are used in the calculations are shown in Tab. 1. The graph of the function $f(R)$ is shown in Fig. 2. The dependence of the ultrasonic attenuation cross-section by air bubbles on the sound wave frequency is shown in Fig. 3. This dependence is obtained for the air bubbles with radius $R = 0.005$ cm.

The existing theories of ultrasonic propagation in liquids with the suspended particles suggest the presence of particles of the same size.

R , cm	0.0003	0.0005	0.001	0.002	0.005	0.010
$f(R)$, cm^{-1}	0.54	2.73	5.45	33.0	54.5	10.8
R , cm	0.015	0.020	0.025	0.030	0.035	0.040
$f(R)$, cm^{-1}	4.9	2.12	1.09	0.65	0.41	0.21

Table 1-1 The values of gas bubble size distribution function.

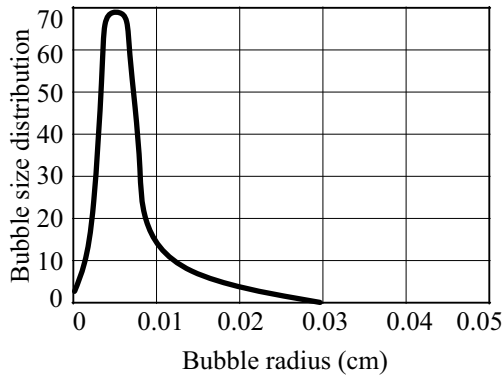


Fig. 1-2 The function of air bubble size distribution.

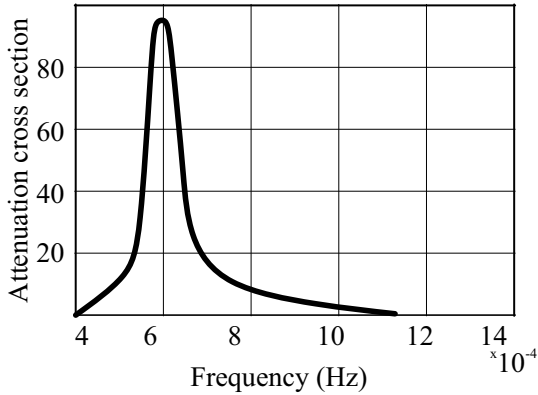


Fig. 1-3 The dependence of the ultrasonic attenuation cross-section by air bubbles on the sound wave frequency, $R = 0.005\text{cm}$.

Since the granulometric characteristic of the crushed material in the pulp has a probability character and considering the variation of gas bubble size distribution, it is interesting to investigate the effect of solid particles and gas bubbles fluctuations (number and size) on the ultrasonic field characteristics.

1.3. The laws of fluctuations influence on the number and size of particles which are suspended in a liquid on the ultrasonic field characteristics

As shown earlier, the ultrasound absorption and scattering by particles which are suspended in a liquid, depend on the acoustic oscillations wavelength. The ultrasound absorption at the low frequencies dominates the scattering (Fig. 1). Therefore, the radiation field is formed mainly of non-scattered acoustic vibrations of these frequencies. However, even at high frequencies, there are areas where the unscattered radiation dominates over the scattered. It takes place at short distances from the radiation source. Otherwise, the scattered radiation contribution becomes significant. From a research point of view of factors affecting the propagation of ultrasound in real pulp, each of these components is of independent interest. Let's assume that a single disc source forms a directed beam of ultrasonic waves (Fig. 4). Such a source of acoustic oscillations can be described by the radiation source density, as follows:

$$S_{\lambda}(\vec{r}, \vec{\Omega}) = \delta(Z - Z_0) \frac{\delta(\cos \nu - 1)}{2\pi} \frac{St(k - \rho)}{\pi a^2}, \quad (1.11)$$

where $\cos \nu \equiv (\vec{\Omega} \cdot \vec{k})$; \vec{k} is the unit vector directed along the Z -axis; $\rho = \sqrt{x^2 + y^2}$; a is the radius of the disc source; Z_0 is the plane coordinate of the disc source; and $St(x)$ is the step function with the property

$$St(x) = \begin{cases} 1, & X > 0 \\ 0, & X \leq 0 \end{cases}. \quad (1.12)$$

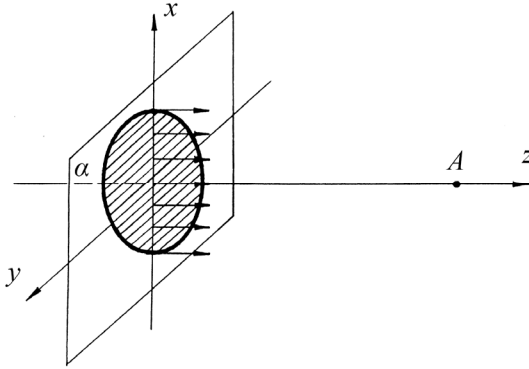


Fig. 1-4 The spatial orientation of the ultrasonic vibrations transducer disc; a is a radius of the transducer.

The unscattered ultrasonic wave intensity is determined by the free term of (1.5) through the radiation source density function:

$$I_{\lambda}^{\circ}(\vec{r}, \vec{\Omega}) = \int_0^{\infty} S(\vec{r} - \xi \vec{\Omega}, \vec{\Omega}) e^{-\tau(\xi, \lambda)} d\xi. \quad (1.13)$$

By substitution (1.11) into the formula, we obtain

$$I_{\lambda}^{\circ}(Z, \rho, \cos \nu) = \frac{\delta(\cos \nu - 1)}{2\pi} \frac{St(a - \rho)}{\pi a^2} \exp\{-\sum(Z - Z_0)\}. \quad (1.14)$$

The detector indications of the ultrasonic waves radiation are proportional to the integral intensity, i.e. the value of:

$$I_{\lambda}(\vec{r}) = \int d\Omega I_{\lambda}(\vec{r}, \vec{\Omega}). \quad (1.15)$$

After integration of (1.14) over the angular variable, we obtain the value of the integral intensity:

$$I_{\lambda}^{\circ}(Z, \rho) = I_{0, \lambda} St(a - \rho) e^{-\Sigma(Z-Z_0)}, \quad (1.16)$$

where $I_{0, \lambda}$ is the wave beam intensity value at the points with coordinate $Z=Z_0$. Later, Z_0 can be set equal to zero. It means that the source is at the origin.

Let's consider the case when the radiation detector is located at the beam axis of the acoustic oscillations. Then the detector response will be proportional to:

$$I_{\lambda}^0(Z) = I_{0, \lambda} e^{-\Sigma Z}. \quad (1.17)$$

Considering (1.1) and (1.4), we can write

$$\Sigma(\lambda) = n_1 \sigma_p(\lambda, R) + n \sigma(\lambda, r), \quad (1.18)$$

where n_1 is the air bubbles concentration; n is the solid particles concentration; $\sigma(\lambda, R)$ is the ultrasonic oscillations attenuation cross-section with the wavelength λ on the air bubble with a radius R ; and $\sigma(\lambda, r)$ is the ultrasonic oscillations attenuation total cross-section with a wavelength λ on the solid phase particle of a radius r .

Practically, the gas phase in the pulp does not contain bubbles of the same radius. Therefore, for the correct evaluation of the air bubbles' influence on the ultrasonic beam attenuation amount, it is necessary to consider the fluctuation of the bubbles number in the volume, as well as the bubble size distribution. The latter is especially important, since the attenuation cross-section on the bubbles has a resonance nature. The same treatment should be carried out for the solid phase particles.

The above situation corresponds to the geometry of the experiment which is shown in Fig. 5. The detector registers the ultrasonic waves, which are passed through the controlled volume V . The fluctuations of the bubbles number in the controlled volume V affect the indication of the detector D .

Let's define the concentration of air bubbles by the number of bubbles N_1 in the volume V :

$$n = \frac{N_1}{V}. \quad (1.19)$$

Since the number of bubbles fluctuates, then N_1 is a random number of the Poisson distribution [8]:

$$P_{N_1}(k) = \frac{\langle N_1 \rangle^k e^{-\langle N_1 \rangle}}{k!}, \quad k = 0, 1, 2, \dots, \quad (1.20)$$

where $\langle N_1 \rangle$ is the average number of N_1 in the volume V , which can be defined by the average value of the concentration \bar{n}_1 :

$$\langle N_1 \rangle = \bar{n}_1 V. \quad (1.21)$$

Let's select only the part which determines the attenuation of ultrasonic oscillations by air bubbles in (1.17):

$$I_\lambda^\circ(Z) = I_\lambda \exp \left\{ -\frac{1}{V} \sum_{i=1}^{N_1} \sigma_p(\lambda, R_i) Z \right\}. \quad (1.22)$$

The response of detector D will be proportional to the value $I_\lambda^\circ(Z)$, averaged over the fluctuations of the number and sizes of bubbles, i.e. proportional to:

$$\langle I_\lambda^\circ(Z) \rangle = I_\lambda \langle \exp \left\{ -\frac{1}{V} \sum_{i=1}^{N_1} \sigma_p(\lambda, R_i) Z \right\} \rangle. \quad (1.23)$$

Let's denote the random variable by ξ :

$$\xi = \exp \left\{ -\frac{1}{V} \sum_{i=1}^{N_1} \sigma_p(\lambda, R_i) Z \right\}. \quad (1.24)$$

Let's use the formula of the total mathematical expectation to define the average value ξ [7]:

$$M_\xi = \sum_{k=0}^{\infty} M \left(\frac{\xi}{k} \right) P_{N_1}(k). \quad (1.25)$$

Here, M_ξ is the mathematical expectation of a random variable ξ , $M(\xi/k)$ is the conditional expectation.

It is easy to show that:

$$M\left(\frac{\xi}{k}\right) = \left[M \exp\left\{-\frac{1}{V} \sigma_p(\lambda, R) Z\right\} \right]^k, \quad (1.26)$$

where:

$$M \exp\left\{-\frac{1}{V} \sigma_p(\lambda, R) Z\right\} - \int_0^\infty \exp\left\{-\frac{Z}{V} \sigma_p(\lambda, R) Z\right\} f(R) dR = \eta_1. \quad (1.27).$$

Here, $f(R)$ is the gas bubble size distribution function.

By substituting (1.20) and (1.27) in (1.25), we obtain:

$$M\xi = \sum_{k=0}^{\infty} \eta_1^k \frac{(n_1 V)^k}{k!} e^{-\bar{n}_1 V} = e^{-\bar{n}_1 V} \exp\{\bar{n}_1 V \eta_1\} = e^{-\bar{n}_1 V(1-\eta_1)}. \quad (1.28)$$

Similarly, considering the fluctuations of the number and sizes of the solid particles, we can obtain the averaged value of the integrated intensity of the ultrasonic vibration, which is passed through a controlled volume of pulp:

$$\langle I_\lambda^0(Z) \rangle = I_{0,\lambda} \exp\left\{-V[\bar{n}_1(1-\eta_1) + \bar{n}(1-\eta)]\right\}, \quad (1.29)$$

where $\eta = \int_0^\infty \exp\left\{-\frac{1}{V} \sigma(\lambda, r) Z\right\} \phi(r) dr$; $\phi(r)$ is the solid phase particle size distribution function, which has the same meaning as the function $f(R)$.

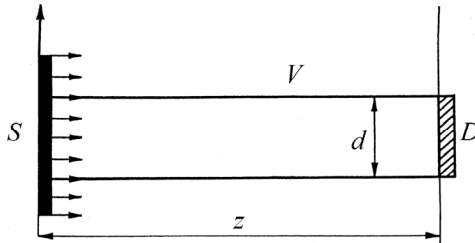


Fig. 1-5 Geometrical interpretation of the measuring channel: S is the source of ultrasonic oscillations; D is the detector; V is the controlled volume; and d is an effective area diameter, which is controlled by the detector.

As can be seen from Fig. 5, the controlled volume V , can be defined by Z

$$V = \frac{\pi d^2}{4} Z. \tag{1.30}$$

In this case, η and η_1 don't depend on the variable Z .

As is known, the intensity of the wave is proportional to the square of the wave amplitude [7], therefore, if we know (1.29), we can proceed to the amplitude dependence:

$$\langle A_\lambda(Z) \rangle = A_{o,\lambda} \exp \left\{ -\frac{1}{2} \frac{\pi d^2}{4} [\bar{n}_1(1-\eta_1) + \bar{n}(1-\eta)] Z \right\}. \tag{1.31}$$

The symbol $\langle \rangle$, as in the previous case, means averaging over the fluctuations of the size and number of solid and gas phase particles.

To investigate the dependence (1.29), it is convenient to go to the new value of α_λ :

$$\alpha_\lambda = \frac{1}{Z} \ln \frac{I_{o,\lambda}}{\langle I_\lambda^\circ(Z) \rangle} = \frac{\pi d^2}{4} [\bar{n}_1(1-\eta_1) + \bar{n}(1-\eta)], \tag{1.32}$$

In conclusion, it should be noted that the heterogeneous medium phase composition is usually defined as a volume fraction of each phase, so in (1.29), (1.31), and (1.32), it is more convenient to pass from the average concentration of the air bubbles number \bar{n}_1 to their volume fraction W . Let's consider this transition in more detail:

$$\begin{aligned} \bar{n}_1(1-\eta_1) &= \bar{n}_1 \cdot \int_0^\infty \left[1 - \exp \left\{ -\frac{4}{\pi d^2} \sigma_p(\lambda, R) \right\} \right] f(R) dR = \\ &= \int_0^\infty \left[1 - \exp \left\{ -\frac{4}{\pi d^2} \sigma_p(\lambda, R) \right\} \right] \frac{WF(R) dR}{4/3\pi R^3} = WQ. \end{aligned} \tag{1.33}$$

In this equation, $WF(R)dR$ determines the volume fraction of the air bubbles whose radii range from R up to $R+dR$.

Function $F(R)$ is associated with $f(R)$ by the ratio:

$$F(R) = \frac{R^3 f(R)}{\int_0^{\infty} R^3 f(R) dR}. \quad (1.34)$$

Thus, according to the latest values, (1.32) can be written as:

$$\alpha_\lambda = \frac{1}{Z} \ln \frac{I_{o,\lambda}}{\langle I_\lambda^\circ(Z) \rangle} = \frac{\pi d^2}{4} [WQ + \bar{n}_1(1-\eta)]. \quad (1.35)$$

When calculating α_λ , the function of solid phase particle size distribution $\varphi(r)$ was corresponded to the beta distribution [12]:

$$\alpha\varphi(X) = \frac{1}{e(\alpha, \beta)} X^{\alpha-1} (1-X)^{\beta-1}, \quad (1.36)$$

where $\alpha = 2\bar{r}$; \bar{r} is the average radius value of the solid phase particles, which are suspended in the liquid; and $e(\alpha, \beta)$ is the beta function.

The dependence of α_λ on the frequency for the different values of α and β is shown in Fig. 6.

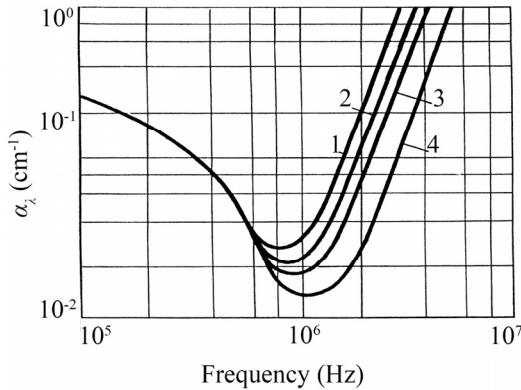


Fig. 1-6 The dependence of α_λ on the frequency for the different parameters of beta distribution: 1 - $\alpha=\beta=1$; 2 - $\beta=2$; 3 - $\alpha=\beta=3$; 4 - $\alpha=\beta=\infty$.

The shaded area corresponds to the change of α_λ in a variation of α and β , from one to infinity. The value α_λ depends on the concentration of solid particles n . The dependence of α_λ on the frequency for various values of n is shown in Fig. 7.

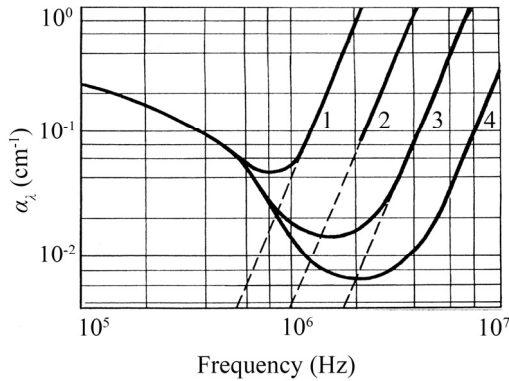


Fig. 1-7 The dependence of α_λ on the frequency for various values of concentration n : 1) $n_1 = 10^4 \text{ cm}^{-3}$; 2) $n_2 = 10^3 \text{ cm}^{-3}$; 3) $n_3 = 10^2 \text{ cm}^{-3}$; 4) $n_4 = 10 \text{ cm}^{-3}$; $r = 0.01 \text{ cm}$.

As can be seen from Fig. 7, in frequency regions where the ultrasound beam attenuation on the solid phase particles dominates over absorption by air bubbles, the effect of the particles concentration is observed.

Thus, with the change of n , the absolute value of α_λ in this frequency region varies, but the slope of graphic dependencies does not change. This fact can be used to determine the concentration of the pulp solid phase particles.

The value α_λ depends not only on the concentration of n , but also on the average particle size, which is seen in Figs. 8 and 9. The dependencies in these figures are obtained for $\alpha = \beta = 3$.

In the case when the value α_λ is determined by the ultrasound attenuation on solid phase particles, the slope curve α_λ does not depend on the average particle radius (in Fig. 8, the dotted lines indicate the slope of the linear portion of the figures).

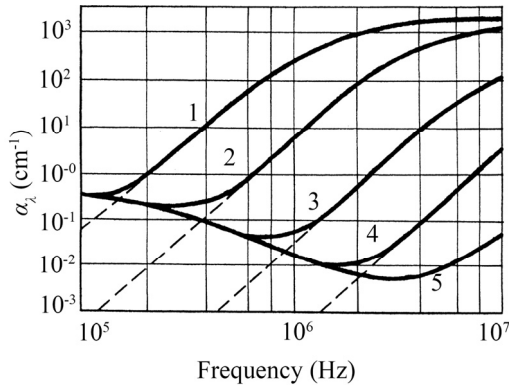


Fig. 1-8 The dependence of α_λ on the frequency for various values of average particle radius: 1) $\bar{r} = 0.1\text{cm}$; 2) $\bar{r} = 0.05\text{cm}$; 3) $\bar{r} = 0.02\text{cm}$; 4) $\bar{r} = 0.01\text{cm}$; 5) $\bar{r} = 0.005\text{cm}$; $n = 10^2\text{cm}^{-3}$; $\alpha = \beta = 3$.

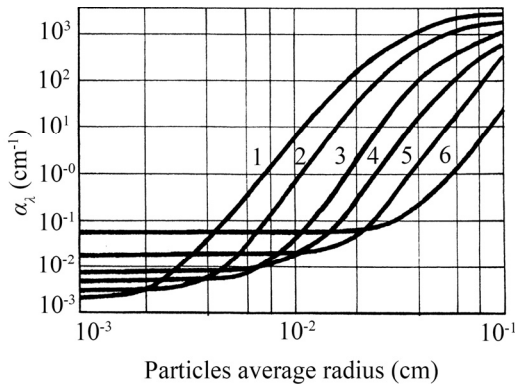


Fig. 1-9 The dependence of α_λ on the average radius of suspended particles for various ultrasonic oscillations frequencies: 1) $\nu_1 = 10^7$ Hz; 2) $\nu_2 = 5 \cdot 10^6$ Hz; 3) $\nu_3 = 2.5 \cdot 10^6$ Hz; 4) $\nu_4 = 1.6 \cdot 10^6$ Hz; 5) $\nu_5 = 10^6$ Hz; 6) $\nu_6 = 5 \cdot 10^5$ Hz; $n = 10^2\text{cm}^{-3}$.

However, this does not prevent determination of the average size, as well as the concentration of suspended particles. This is because the average particle size determines the frequency V_k , in which the components of absorption and scattering on the solid particles become equal to V_k . Therefore, by this value we can view the average particle size.

The components of $\sigma_{\lambda i}$, caused by the ultrasonic oscillations attenuation by air bubbles, while the absorption and scattering by solid phase particles suspended in a liquid are shown in Fig. 10.

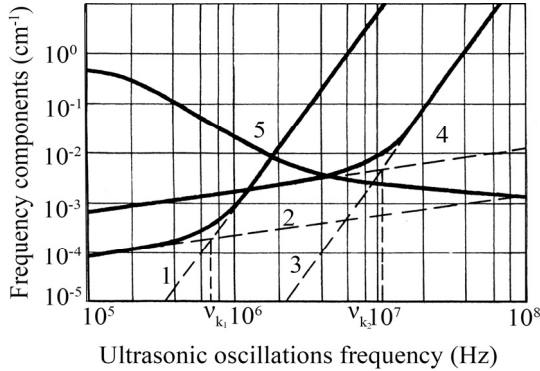


Fig. 1-10 The dependence of frequency components σ_i on the ultrasonic oscillations frequency: 1, 3 - the components due to scattering on the solid particles; 2,4 - the components due to the absorption of solid particles; 5 - the components of attenuation by air bubbles; 1, 2 - $\bar{r} = 0.01\text{cm}$; 3, 4 - $\bar{r} = 0.001\text{cm}$.

The frequencies V_{k1} and V_{k2} , which should be used for the measurement of solid particles in the pulp with the average 10^{-2} and 10^{-3}cm , are also shown. The values of the frequency V_k are independent of the particles concentration.

1.4. Evaluation of the scattered ultrasonic waves intensity

We have shown earlier that with the frequency increase, the ultrasonic waves scattering cross-section on the solid particles increases sharply. In this case, the radiation field is formed by the unscattered, as well as scattered, waves. The correct calculation of the scattered waves radiation field is challenging. Let's restrict the analysis of singly scattered ultrasonic waves contribution to estimate the main characteristics of the scattered radiation.

The intensity of the singly scattered waves can be found from (1.5):

$$I_{\lambda}^s(\vec{r}, \vec{\Omega}) = \int d\vec{r}' \int d\vec{\Omega}' \sum_s (\vec{\Omega}' \rightarrow \vec{\Omega}) \frac{e^{-\tau(\vec{r}', \vec{r}, \lambda)}}{|\vec{r} - \vec{r}'|} \delta\left(\vec{\Omega} - \frac{\vec{r} - \vec{r}'}{|\vec{r} - \vec{r}'|}\right) I_{\lambda}^s(\vec{r}', \vec{\Omega}'). \quad (1.37)$$

We will be interested in the integrated intensity of singly scattered waves, i.e. the value of:

$$I_{\lambda}^s(\vec{r}) = \int_{4\pi} d\Omega(\vec{r}, \vec{\Omega}). \quad (1.38)$$

By substituting the right side of (1.37) in (1.38) and after integrating, we obtain:

$$I_{\lambda}^s(\vec{r}) = \int d\vec{r}' \int d\vec{\Omega}' \sum_s \left(\vec{\Omega}' \rightarrow \frac{\vec{r} - \vec{r}'}{|\vec{r} - \vec{r}'|} \right) \frac{e^{-\tau(\vec{r}', \vec{r}, \lambda)}}{|\vec{r} - \vec{r}'|} \cdot I_{\lambda}^s(\vec{r}', \vec{\Omega}'). \quad (1.39)$$

Let's estimate this value at point A on the axis of the ultrasonic beam (Fig. 4). Considering (1.14), we can write (1.39) in the cylindrical coordinate system:

$$I_{\lambda}^s(Z) = 2\pi \int_0^Z dZ' \int_0^a d\rho' \cdot \rho' I_{\sigma, \lambda} e^{-\Sigma Z'} \sum_s (\mu) \frac{e^{-\Sigma \xi}}{\xi^2}, \quad (1.40)$$

where $\xi = |\vec{r} - \vec{r}'| = \sqrt{(Z - Z')^2 + \rho'^2}$; $\mu = \vec{k} \cdot \frac{(\vec{r} - \vec{r}')}{|\vec{r} - \vec{r}'|}$; \vec{k} is the unit vector directed along the Z -axis.

To calculate (1.40) we should make some approximations. First, let's consider the case when $Z \gg a$, then $\xi \approx Z - Z'$. Secondly, we assume that scattering by particles is isotropic, then:

$$\sum_s (\vec{\Omega} \rightarrow \vec{\Omega}') = \frac{n\sigma_s}{4\pi}, \quad (1.41)$$

where σ_s is the total scattering cross-section.

Taking into account these approximations, by integration in (1.40), we obtain:

$$I_{\lambda}^s(Z) = \frac{n\sigma_s}{4} e^{-\Sigma(\lambda)Z} I_{0, \lambda} \left\{ Z \ln\left(1 + \frac{a^2}{Z^2}\right) + 2a \cdot \text{arctg} \frac{Z}{a} \right\}. \quad (1.42)$$

Let's introduce the quantity β_v :